DETECTION AND CHARACTERIZATION OF THE SUB-KM ASTEROID POPULATION IN THE MAIN ASTEROID BELT. Tushar Mittal[1], Danny Goldstein[2], and Peter Nugent[2]. [1](Department of Earth and Planetary Science, University of California Berkeley, Berkeley, CA; tmittal2@berkeley.edu), [2](Department of Astronomy, University of California Berkeley, Berkeley, CA).

Introduction: The coagulation and fragmentation of small bodies to form planetesimals is an important step in planet formation. The disruption criterion for collisions among various sized objects and at different velocities directly the size distribution in a collisional cascade [1] and thus impacts the evolution and growth of the larger proto-planets as well as the dust production in proto-planetary disks and debris disks.

The criterion for catastrophic collisions in which the largest surviving fragment has less than half of the target's mass, is typically represented by the critical kinetic energy of the projectile per unit mass of the target (Q_D*). Q_D* generally decreases with increasing diameter for asteroids less than ~0.1 km ('strength-scaled regime') and increases with increasing diameter for the larger asteroids ('gravity-scaled regime') with a transition zone at .1-1 km sized asteroids [2]. Since Q_D* curves have been estimated theoretically and through numerical simulations for target bodies with different composition and internal structure, measurement of the small body population in the Asteroid Main Belt (2.5 - 3.5 AU) can be used to test the model predictions, especially in the Q_D* transition region. In addition, a high resolution analysis of the size distribution of Main Belt Asteroids (MBAs) can provide useful insight into the collisional and dynamical evolution of MBAs, and the production rate of meteoroids, and near-Earth asteroids and the cratering rates on the surface of inner planets.

The size distribution of MBAs down to sub-km size has been estimated by a few previous surveys with ground-based telescopes such as the Subaru Main Belt Asteroid Survey (SMBAS; [3],[4]), and the Sub-Kilometer Asteroid Diameter Survey ([5]) (See Figure 1). The objective of our study is to use novel analysis techniques to push the detection limit further (~100 m-scale; r magnitude > 24.5) in order to better constrain the population of asteroids corresponding to the transition region in Q_D* and also to characterize the population using statistical models to understand the accretion and collisional evolution of the solar system.

Analysis Technique: Due to PSF broadening and orbital phase lag, objects in our target population appear as extremely faint tracklets in single-exposure images, even with large, ground-based telescopes. Preliminary photometric simulations of few 100m targets using DECam[6] systematics show that tracklets of objects with representative projected orbital speeds (20''/hr. - 40''/hr) fall below a signal-to-noise ratio of 1.0 in 300s r-band exposures, even under optimal observing conditions. To detect these faint objects, we have developed a specialized pipeline that includes a differencing code, two independent methods for object detection, and multiple routines for false source removal.

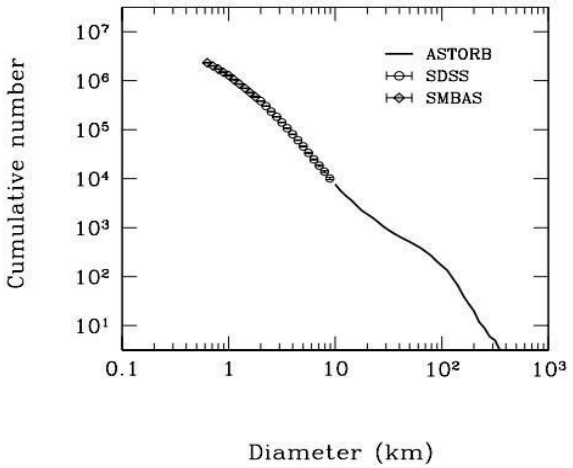

Figure 1: The cumulative size distribution of main-belt asteroids. From [4]

The pipeline begins with a co-addition routine that creates deep reference images of target fields, using archival photometry. These reference images are aligned with new single-exposure images. A subsequent routine identifies point sources common to both images, which are then eliminated by a subtraction routine. Importantly, this technique preserves the sky background of input images.

The resulting subtracted images are subjected to two independent procedures for object detection. In procedure 1 ("the convolutional procedure"), we follow [7] in generating a grid of orbital parameters α, β, and *d* (where α and β are the orthogonal components of the projected orbital speed, and *d* is the distance parameter as defined in [7]), that completely specify the set of asteroid orbits differentiable at the instrumental pixel scale. We first synthesize a convolution kernel based on the tracklet shape at each grid point, and then convolve it with our input image. Image tracklets that match the kernel shape are amplified by as much as 10x, while other image patterns due to noise are significantly de-weighed. Finally, we run SExtractor[8] on the convolved image to detect the asteroids.

In procedure 2 ("the iterative procedure"), we generate a series of trajectories along which to shift input images using a asteroid motion model based on the grid in procedure 1. For a given input image, we divide each trajectory into steps, then iteratively shift the input image along the trajectory, step-by-step. After each it-

eration, we subtract the input image from itself to form a set of subtraction image layers in memory. Finally, we re-align the layers and co-add them into a single image. This process amplifies the signal of observed tracklets, which appear as distended PSFs detectable by SExtractor. Point sources are negated and easily identifiable.

When a source is detected by both the procedures, it continues onward to false source removal. Some sources that reach this point may be variable stars mistaken for asteroids by the assumption of a slow orbit and non-perfect reference image subtraction. Accordingly, false source removal begins with the removal of known variable stars, using a star catalog. Next, we compare the multicolor magnitudes of detected objects with non-thermal asteroid models, throwing away poor fits. Finally, we perform tracklet detection across intra-night and inter-night images, removing detections that do not reasonably follow extracted orbits across exposures. An important aspect of the complete algorithm is that a single exposure image is used to detect faint tracklets. We also perform additional image stacking using the shifted intra-night images to detect even fainter objects.

Applications: By combining our method with photometry from large-scale observational surveys, a previously unobserved population of solar system objects can be characterized, both statistically and individually. In particular, photometry from existing deep surveys like the SMBAS as well as other archival imaging surveys of the ecliptic plane by large telescopes can be used for the detection of specific objects. On the other hand, wide-field surveys like the ongoing Dark Energy Survey (5,000 sq. deg.)[9], revisit target fields multiple times nightly, exposing in multiple filters (grizY). These repeated exposures facilitate intra-night object tracking, and the color information is useful for false source rejection besides spectral classification of detected asteroids. Although DECam dataset probes shallower than Subaru or Keck, its abundant photometric data will substantiate a debiased statistical characterizations of the smaller Main Belt population. Currently, we are pursuing each of these applications, both as members of the Dark Energy Survey and with public SMBAS data. Since our search algorithm is computationally very intensive, we plan to utilize the supercomputing resources at NERSC for this study.

References: [1] Pan, M. & Schlichting, H. E. (2012). *ApJ*, 747(2), 113. [2] Stewart, S. T. and Leinhardt, Z. M. *ApJL* 691.2 (2009): L133. [3] Yoshida, F., and T. Nakamura. Planetary and Space Science 55.9 (2007): 1113-1125. [4] Terai, T. et al. *ApJ* 146.5 (2013): 111. [5] Gladman, B. J., et al. Icarus 202.1 (2009): 104-118. [6] DePoy, D. L., et al. International Society for Optics and Photonics, 2008. [7] Bernstein, G. M., et al. *ApJ* 128.3 (2004): 1364. [8] Bertin, E., and S. Arnouts. Astronomy and Astrophysics Supplement Series 117 (1996): 393-404. [9] Collaboration, T. D. E. S. "The dark energy survey." (2005).

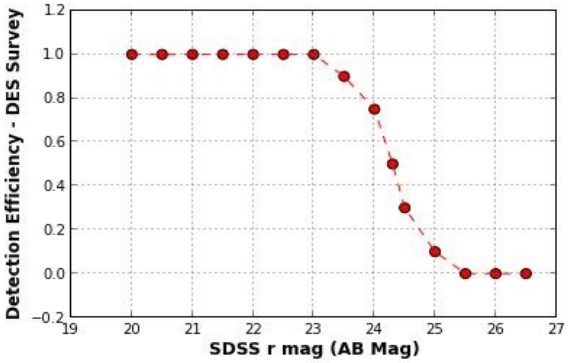

Figure 2: Preliminary detection efficiency η(r) for moving objects as a function of apparent r magnitude (DES Survey Characteristics) using realistic sky noise. The detection efficiency reduces with motion velocity due to the decrease in flux density.

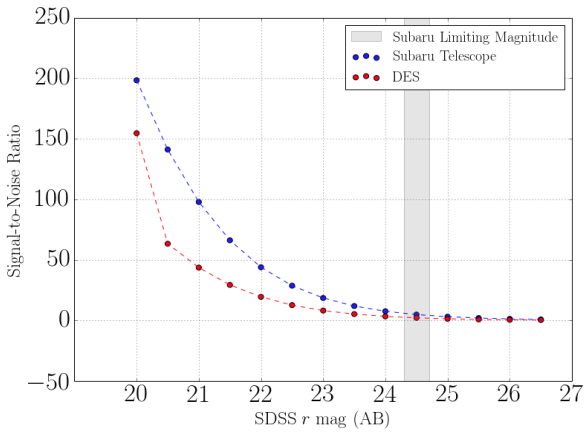

Figure 3: Signal-to-Noise ratio using Subaru and DES exposure time calculators. The Magnitude limit for detection from [3] is shown on the plot. Based on our Preliminary analysis using fake sources, we expect improvements in sensitivity on the order of .5 - 1 magnitude.